DOI: 10.1002/chem.200500503

Induction and Inhibition of Preferential Enrichment by Controlling the Mode of the Polymorphic Transition with Seed Crystals

Rui Tamura,* Masayuki Mizuta, Shinsuke Yabunaka, Daisuke Fujimoto, Tomomi Ariga, Shinichiro Okuhara, Naohiko Ikuma, Hiroki Takahashi, and Hirohito Tsue[a]

Abstract: Both induction and inhibition of "preferential enrichment", an unusual symmetry-breaking enantiomeric-resolution phenomenon observed upon simple recrystallization of a certain kind of racemic crystals from organic solvents, have been successfully achieved by controlling the mode of the polymorphic transition during crystallization with appropriate seed crystals. Such control of the polymorphic transition can be interpreted in terms of a novel phenomenon consisting of 1) the adsorption of prenucleation aggregates, 2) the heterogeneous nucleation and crystal growth of a metastable crystalline form, and 3) the subsequent polymorphic transition into the more stable form; these three processes occur on the same surface of a seed crystal. We refer to this phenomenon as an "epitaxial transition", which has been confirmed by means of in situ attenuated total reflection (ATR) FTIR spectroscopy in solution and the solid state, differential scanning calorimetry (DSC) measurements of the deposited crystals, and X-ray crystallographic analysis of the single crystals or the direct-space approach employing the Monte Carlo method with the Rietveld refinement for the structure solution from the powder X-ray diffraction data.

Keywords: chiral resolution · crystal growth · epitaxial transition · polymorphism · preferential enrichment

Introduction

In 1996 we reported the first instance in which enantiomeric resolution by simple recrystallization of a racemic crystal from organic solvents was feasible;[1] this unusual symmetry-breaking enantiomeric-resolution phenomenon was referred to as "preferential enrichment".[2] Since then, more than ten structurally analogous racemic samples have been found to exhibit the same phenomenon that can give both enantiomers in high enantiomeric excess (*ee*) and quantity by a simple operation.[3–8] Mechanistically, it has been revealed that preferential enrichment is a secondary, dynamic enantiomeric-resolution phenomenon caused by the solvent-assisted solid-to-solid transformation of a metastable γ-polymorphic form into a thermodynamically stable δ form (or ε form in a specific case) during crystallization from the supersaturated solution of a certain kind of racemic mixed crystals (i.e., solid solutions or pseudoracemates) composed of the two enantiomers (Figure 1).[3,7,8,9] Accordingly, a certain mode of polymorphic transition has turned out to be crucial to the occurrence of preferential enrichment. Therefore, on the basis of the elucidated mechanism of this unique polymorphic transition observed for a series of racemic samples that can show preferential enrichment, it may become possible to induce preferential enrichment for their structurally analogous racemic samples, which cannot exhibit this phenomenon, by controlling the mode of the polymorphic transition.

Control of polymorphism giving a desired polymorphic form by crystallization has been a long-standing subject to be realized in connection with the development of crystal engineering, closely associated with organic materials science.[10] Of the various methods contrived thus far—such as changing the crystallization conditions,[11] seeding with a

[a] Prof. R. Tamura, M. Mizuta, S. Yabunaka, Dr. D. Fujimoto, T. Ariga, S. Okuhara, N. Ikuma, Dr. H. Takahashi, Dr. H. Tsue
Graduate School of Human and Environmental Studies
Kyoto University
Kyoto 606-8501 (Japan)
Fax: (+81) 75-753-7915
E-mail: tamura-r@mbox.kudpc.kyoto-u.ac.jp

Supporting information for this article is available on the WWW under http://www.chemeurj.org/ or from the author. It contains 1) crystal structure information files (CIFs), 2) observed, calculated, and difference profiles of the Rietveld refinement, and 3) crystal structures, obtained by the computational direct-space approach for the δ_1 form of (±)-**1a** (alternative name, $NNMe_3$–OMe), the δ_1 form of (±)-**1b** ($NCMe_3$–OMe), and the κ and δ_1 forms of (±)-**1c** ($NBMe_3$–OMe).

 © 2006 Wiley-VCH Verlag GmbH & Co. KGaA, Weinheim WILEY InterScience DISCOVER SOMETHING GREAT

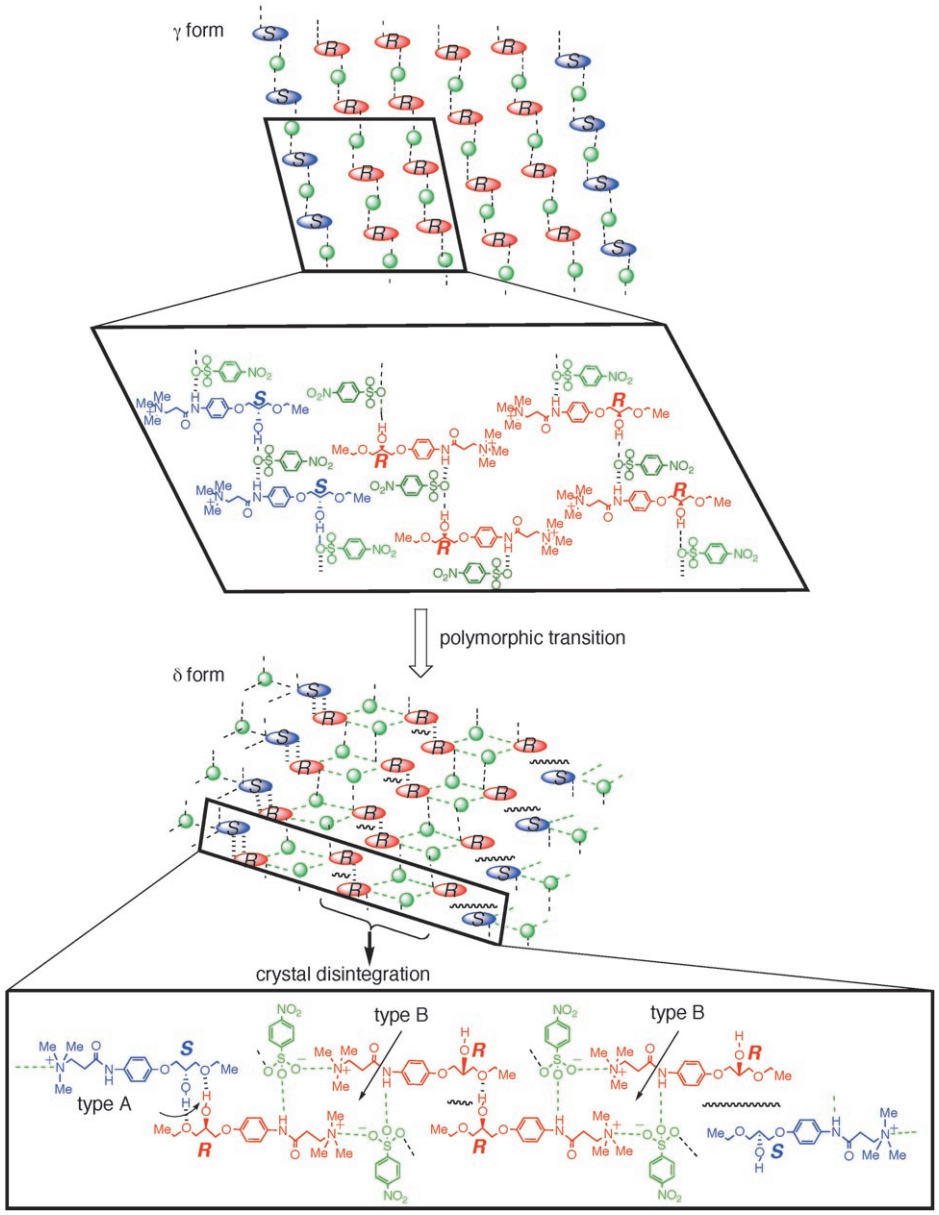

Figure 1. Polymorphic transition of the metastable γ form into the stable δ form, which is essential for the occurrence of preferential enrichment for (±)-**2a**. This is a case in which an even number (four in this case) of homochiral *R* chains are surrounded by two *S* chains in the γ-form crystal, resulting in partial crystal disintegration after polymorphic transition. The ellipsoid and circle indicate the chiral long-chain cation and achiral sulfonate ion, respectively.

crystal of the desired structure,[12] or adding impurities or additives to inhibit the nucleation or the crystal growth of an undesired polymorphic form[13]—induced crystallization with adequate seed crystals possessing a target crystal structure seems to be the most straightforward and promising for designed crystallization.[9,12,14,15] Such control of polymorphism by seeding is usually accounted for by the heterogeneous nucleation and the subsequent epitaxial growth on the crystalline surface. If the molecular packing mode in the incipient crystal grown on the crystalline surface is thermodynamically unstable, the subsequent polymorphic transition should occur on the surface too. Thus far, however, no report concerning the control of the bulk polymorphic transition by seeding with appropriate crystals has been documented, although understanding of the mechanism of the polymorphic transition occurring during crystallization has advanced.[1,16,17]

With this situation in mind, we have focused on the terminal methoxy derivatives ((±)-**1a**, (±)-**1b**, (±)-**1c**) of the prototypic ammonium sulfonates ((±)-**2a**, (±)-**2b**, (±)-**2c**) that have shown preferential enrichment,[4,5,7] because whether (±)-**1a**–(±)-**1c** show preferential enrichment or not depends only on the kind of electron-withdrawing group situated at the *para* position of the benzenesulfonate ion (Scheme 1 and Table 1). Consequently, we have found that addition of stable δ-form seed crystals of (±)-[2-[4-(3-methoxy-2-hydroxypropoxy)phenylcarbamoyl]ethyl]trimethylammonium *p*-nitrobenzenesulfonate ((±)-**1a**), which can easily show preferential enrichment (Figure 2), to the supersaturated solution (in EtOH) of the *p*-chlorobenzenesulfonate derivative ((±)-**1b**), which does not show this phenomenon by itself,[4] can explicitly induce preferential enrichment for (±)-**1b** (Table 1 and Figure 11, see below). Conversely, seeding the supersaturated solution of (±)-**1a** in EtOH with the stable δ_1-form crystals of (±)-**1b** has been found to completely inhibit the occurrence of preferential enrichment for (±)-**1a** (Table 1). More interestingly and unexpectedly, it has been observed that seeding with the same δ_1-form crystals of (±)-**1b** in EtOH induces preferential enrichment for the *p*-bromobenzenesulfonate derivative ((±)-**1c**), which does not show this phenomenon by itself (Table 1 and Figure 15, see below).

Here we report the details of these preferential-enrichment experiments and discuss the mode of the controlled polymorphic transition during crystallization of these samples in terms of a new phenomenon, "epitaxial transition", comprising the heterogeneous nucleation and crystal growth

 © 2006 Wiley-VCH Verlag GmbH & Co. KGaA, Weinheim

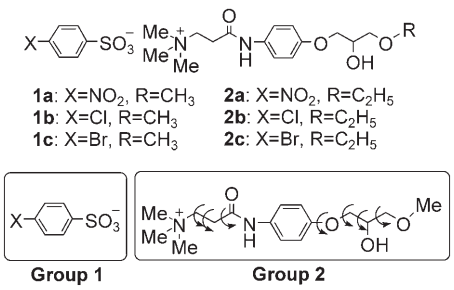

Scheme 1. Ammonium sulfonates, grouping, and seven variable torsional angles for the structure solution of the δ_1 form of (±)-**1a**, the δ_1 form of (±)-**1b**, and the κ and δ_1 forms of (±)-**1c**.

Table 1. Induction or inhibition of preferential enrichment by mutual seeding for (±)-**1a**–(±)-**1c**.[a]

	Solubility in EtOH [mg mL^{-1}]	Without seeding[b]	Seed crystal[c] (±)-**1a** δ form	(±)-**1b** δ_1 form	(±)-**1c** κ form
(±)-**1a**	12.9	yes[d,e] (γ to δ)[h]	acceleration[f] (γ to δ)[h]	inhibition[g] (γ to δ_1)[h]	no effect
(±)-**1b**	59.1	no[i] (γ to δ_1)[h]	induction[j,k] (γ to δ, then δ_1)[h]	–	no effect
(±)-**1c**	19.9	no[i] (γ to κ)[h]	no effect	induction[j,l] (γ to δ, then δ_1)[h]	–

[a] 10-, 3-, and 5-fold supersaturated solutions were used for recrystallization of (±)-**1a**–(±)-**1c** in EtOH, respectively. [b] Recrystallization was carried out without seed crystals. [c] 5 wt% of seed crystals were added. [d] Preferential enrichment occurred. [e] See Figure 2. [f] Preferential enrichment was accelerated. [g] Preferential enrichment was completely inhibited by seeding. [h] Mode of polymorphic transition. [i] Preferential enrichment did not occur. [j] Preferential enrichment was induced by seeding. [k] See Figure 11. [l] See Figure 15.

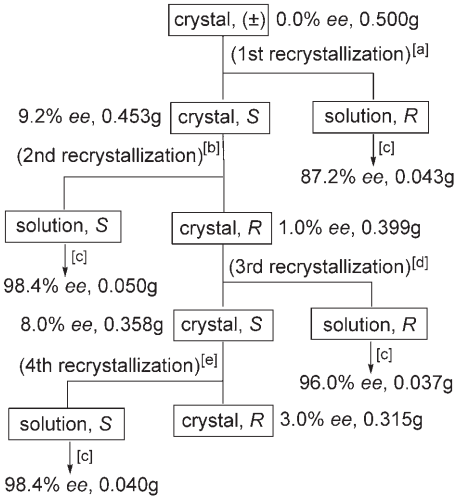

Figure 2. Preferential enrichment of **1a**. The *ee* values were determined by HPLC analysis (see the Experimental Section). Conditions: [a] EtOH (4.0 mL) at 25 °C for 1 day, then at 5 °C for 4 days. [b] EtOH (3.5 mL) at 25 °C for 1 day, then at 5 °C for 4 days. [c] Removal of the solvent by evaporation. [d] EtOH (3.0 mL) at 25 °C for 1 day, then at 5 °C for 4 days. [e] EtOH (2.8 mL) at 25 °C for 1 day, then at 5 °C for 4 days.

of a metastable crystalline form and the subsequent polymorphic transition into the more stable form, both of which occur on the same columnar surfaces of the seed crystals.

Results and Discussion

Preferential-enrichment experiments and X-ray crystal structures for (±)-1a–(±)-1c: We have already reported that (±)-**2a**–(±)-**2c** show preferential enrichment,[4,5,7] whereas (±)-**1b**, the terminal methoxy derivative of (±)-**2b**, was unable to do so.[4] To shed light on such an unexpected relationship between the molecular structure and the occurrence of preferential enrichment, we have prepared (±)-**1a** and (±)-**1c** and have recrystallized them from EtOH under the standard preferential-enrichment experimental conditions. Consequently, (±)-**1a** has successfully exhibited preferential enrichment (Figure 2), whereas (±)-**1c** has failed to do so similarly to (±)-**1b** (Table 1). It is surprising that such a minor molecular modification exerts a primary influence on the occurrence of preferential enrichment. Therefore, to clarify the cause, we first compared the crystal structures of the stable forms of (±)-**1a**–(±)-**1c** with those of (±)-**2a**–(±)-**2c**. We already reported that the crystal structures of the stable forms of (±)-**2a**–(±)-**2c** belong to a δ form (Figure 1),[4,5,7] whereas that of (±)-**1b** adopts a δ_1 form that is partly similar to a δ form (Figure 3 and Table 2).[4] Single crystals of the two new compounds, (±)-**1a** and (±)-**1c**, suitable for X-ray crystallographic analysis were obtained by recrystallization from *i*PrOH.

The crystal structure of (±)-**1a** has been found to be a δ form as expected; it has orientational disorder at the position of the hydroxy group on an asymmetric carbon atom with the occupancy factors of 0.721 and 0.279, as commonly observed for compounds showing preferential enrichment (Figure 4 and Table 2).[4–7] The decisive difference in crystal structure between the δ form of (±)-**1a** and the δ_1 form of (±)-**1b** lies in the mode of interchain interactions between analogous heterochiral one-dimensional (1D) chains, which are composed of two types of centrosymmetric cyclic dimers (type A and type B) (Figures 3 and 4). Type A is formed by the hydrogen bonds between two hydroxy groups and two ethoxy oxygen atoms (O···O distance: 2.67 and 2.903 Å for **1a** and **1b**, respectively) in a pair of *R* and *S* molecules, whereas type B is formed by 1) the hydrogen bond between an oxygen atom of a sulfonate ion and the nearest amide NH (O···N distance: 2.937 and 2.874 Å for **1a** and **1b**, respectively) and 2) the electrostatic interaction between another oxygen atom of the same sulfonate ion and the ammonium nitrogen atom in the neighboring long-chain cation ($O^-\cdots N^+$ distance: 4.135 and 3.787 Å for **1a** and **1b**, respectively). In the δ form of (±)-**1a**, each heterochiral 1D chain interacts with two adjacent chains by another weak electro-

 © 2006 Wiley-VCH Verlag GmbH & Co. KGaA, Weinheim

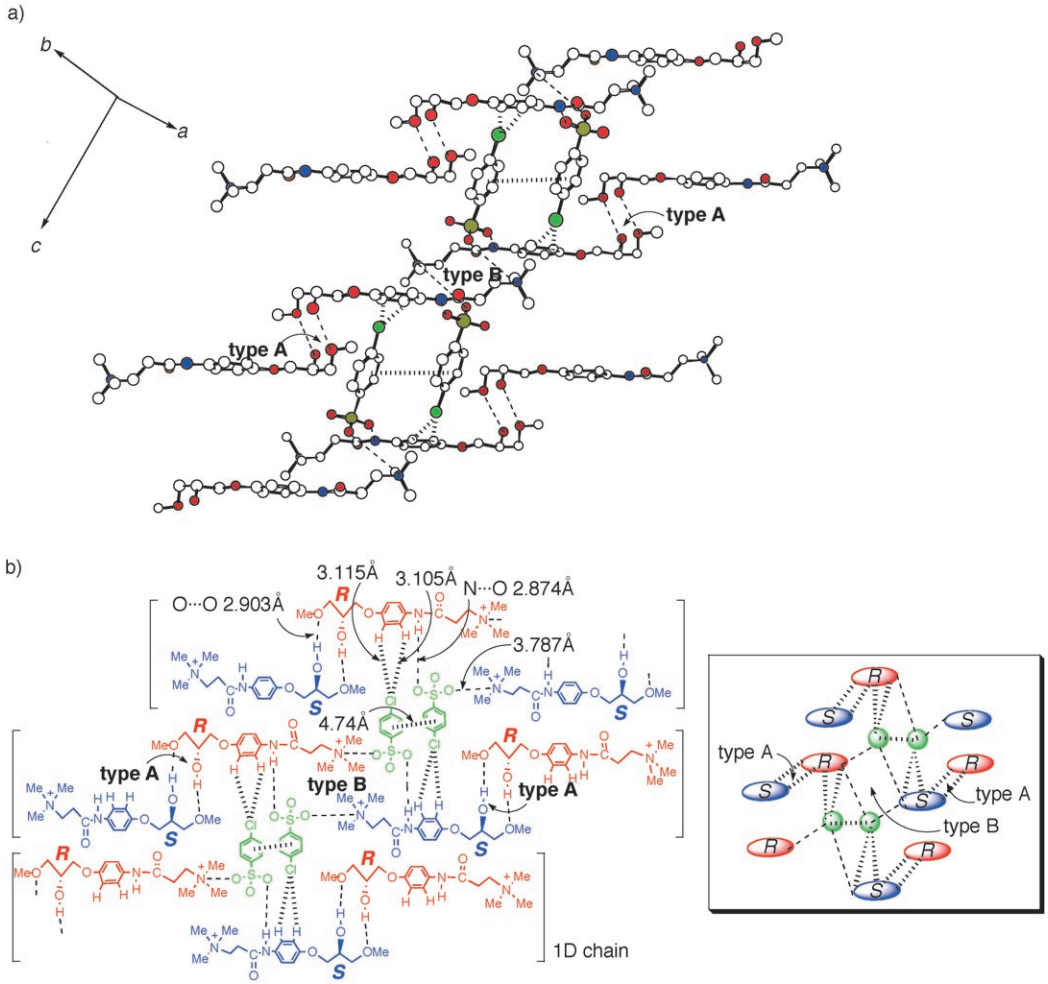

Figure 3. a) Crystal structure of the δ_1 form of (±)-**1b**. The C, O, N, S, and Cl atoms are represented by white, red, blue, yellow, and green circles, respectively. b) Schematic representation of the intermolecular interactions in the crystal. The ellipsoid and circle in the inset indicate the long-chain cation and sulfonate ion, respectively. The dashed lines show the intermolecular hydrogen bonds, electrostatic interactions, π–π interactions, and CH/Cl interactions.

static interaction between the third oxygen atom of the same sulfonate ion and the ammonium nitrogen atom ($O^-\cdots N^+$ distance: 3.906 Å) in the adjacent chain, eventually forming a weak two-dimensional (2D) sheet structure (Figure 4). On the other hand, in the δ_1 form of (±)-**1b** the interplay of two interchain interactions is seen (Figure 3); one is the relatively strong slipped-parallel π–π stacking (interplanar distance: 3.54 Å; intercentroid distance: 4.74 Å; the shortest $C(sp^2)\cdots C(sp^2)$ distance: 3.61 Å) between the benzene rings of the nearest two *p*-chlorobenzenesulfonate groups, and the other is the weak $C(sp^2)H\cdots Cl$ contacts (H···Cl distances: 3.105 and 3.115 Å) between the chlorine atom of the *p*-chlorobenzenesulfonate group and two vicinal hydrogen atoms on the benzene ring of the neighboring long-chain cation, consequently forming a solid 2D sheet structure.[4,18] These fairly strong interchain interactions must be responsible for the nonoccurrence of preferential enrichment with respect to (±)-**1b**, because the subsequent crystal disintegration that is necessary to cause preferential enrichment cannot occur.[3,7,8]

The X-ray diffraction (XRD) patterns and differential scanning calorimetry (DSC) characteristics of (±)-**1a** and (±)-**1b** crystallized from EtOH have been found to be identical to those of the same compounds crystallized from *i*PrOH, indicating that the δ and δ_1 forms are their respective stable forms.[3,7,8]

The crystal structure of (±)-**1c** crystallized from *i*PrOH turned out to be an unexpected γ form (Figure 5 and Table 2), which is believed to be a metastable key-intermediate polymorph and to easily undergo the subsequent polymorphic transition inducing preferential enrichment (Figure 1).[3,7] Indeed, when (±)-**1c** was recrystallized from EtOH, a more stable polymorphic form was obtained as a monophasic powder sample after the swift polymorphic transition of the initially formed γ form on contact with the solvent (Figure 6), but unexpectedly, preferential enrichment never occurs.

To unveil the reason for this, the crystal structure of this new polymorph of (±)-**1c** obtained from EtOH has been solved from its powder XRD data, by using the direct-space

 © 2006 Wiley-VCH Verlag GmbH & Co. KGaA, Weinheim

Table 2. X-ray analytical data for the polymorphs of (±)-**1a**, (±)-**1b**, and (±)-**1c**.

	(±)-**1a**[a]	(±)-**1a**[b]	(±)-**1b**[a,c]	(±)-**1b**[b]	(±)-**1c**[a]	(±)-**1c**[b]	(±)-**1c**[b]
crystal form	δ form[d] 0.721:0.279[h]	δ_1 form[e]	δ_1 form[d]	δ_1 form[f] 0.70:0.30[h]	γ form[d]	κ form[g]	δ_1 form[e] 0.70:0.30[h]
crystal system	triclinic	triclinic	triclinic	triclinic	triclinic	monoclinic	triclinic
space group	$P\bar{1}$	$P\bar{1}$	$P\bar{1}$	$P\bar{1}$	$P\bar{1}$	$P2_1/c$	$P\bar{1}$
a [Å]	8.935(1)	8.297	8.2981(4)	8.292	9.2122(7)	14.893	8.272
b [Å]	9.825(2)	11.203	11.224(1)	11.229	9.4590(5)	8.806	11.237
c [Å]	14.850(2)	14.957	14.568(2)	14.605	15.8841(12)	20.378	14.739
α [°]	106.07(1)	99.39	98.249(9)	98.37	90.075(3)	–	98.62
β [°]	96.157(9)	93.69	94.35(1)	94.28	90.075(5)	109.349	94.21
γ [°]	92.04(2)	111.16	110.756(5)	110.73	103.232(5)	–	110.60
V [Å^3]	1242.6(3)	1267.7	1243.7(2)	1246.5	1347.4(2)	2522.3	1256.1
Z	2	2	2	2	2	4	2
ρ_{calcd} [g cm^{-3}]	1.372	–	1.343	–	1.349	–	–
$2\theta_{max}$	135.8	–	135.9	–	57.5	–	–
reflns measured	4826	–	3997	–	12882	–	–
observed reflns [$I>3\sigma$(I)]	3418	–	1324	–	2285	–	–
parameters	354	–	328	–	328	–	–
$\mu_{K\alpha}$ [cm^{-1}]	16.47	–	25.23	–	16.48	–	–
R[i]	0.076	0.079[j]	0.061	0.048[j]	0.098	0.078[j]	0.078[j]
R_w[k]	0.128	0.099[l]	0.088	0.063[l]	0.170	0.120[l]	0.102[l]
GOF	0.916	–	0.927	–	0.996	–	–
residual density [e Å^{-3}]	+0.75/−0.48	–	+0.67/−0.22	–	+0.996/−0.81	–	–

[a] X-ray crystallographic analysis. [b] The crystal structure solved from the XRD data by the Monte Carlo method with subsequent Rietveld refinement. [c] Reduced unit-cell parameters of the published structure quoted from ref. [4]. [d] Obtained by recrystallization from *i*PrOH without seed crystal. [e] Obtained by recrystallization from EtOH with the δ_1-form seed crystals of (±)-**1b**. [f] Obtained by recrystallization from EtOH with the δ-form seed crystals of (±)-**1a**. [g] Obtained by recrystallization from EtOH without seed crystal. [h] Occupancy factors assigned to the position of the hydroxy group on an asymmetric carbon atom on account of the orientational disorder. [i] R value: $R=\Sigma||F_o|-|F_c||/\Sigma|F_o|$ for $I>3.0\sigma(I)$ data. [j] R_p values: $R_p = [\Sigma|cY^{sim}(2\theta_i)-I^{exp}(2\theta_i)-Y^{back}(2\theta_i)|/\Sigma|I^{exp}(2\theta_i)|$. [k] R_w value: $R_w = [\Sigma w(|F_o|-|F_c|)^2/\Sigma w|F_o^2|]^{1/2}$. [l] R_{wp} value: $R_{wp} = [(\Sigma w_i(cY^{sim}(2\theta_i)-I^{exp}(2\theta_i)-Y^{back}(2\theta_i))^2)/\Sigma w_i(I^{exp}(2\theta_i))^2]^{1/2}$.

approach with the Monte Carlo method and the subsequent Rietveld refinement (see Figure S1 in the Supporting Information).[3,9,19,20] Compound (±)-**1c** was found to be a new type (κ form) consisting of a heterochiral 2D sheet structure, which is quite different from the δ form essential for preferential enrichment to occur (Figure 7 and Table 2).[5,7] This κ-form crystal structure is characterized by a heterochiral 1D chain along the *c* axis, which is formed by 1) two kinds of intermolecular hydrogen bonds between the hydroxy group and the nearest amide NH (O···N distance: 3.156 Å) and between the same hydroxy group and an oxygen atom of the nearest sulfonate group (O···O distance: 2.524 Å) and 2) the O···Br contact (O···Br distance: 3.475 Å) arising from the Coulombic donor–acceptor interaction between the methoxy oxygen atom and the nearest bromine atom.[21] Furthermore, these heterochiral 1D chains interact with each other in a parallel way along the *b* axis by the electrostatic interaction between another oxygen atom of the same sulfonate ion and the nearest ammonium nitrogen atom in the neighboring chain ($O^-\cdots N^+$ distance: 3.796 Å), eventually forming a solid heterochiral 2D sheet structure on the *bc* plane. It is most likely that the O···Br Coulombic donor–acceptor attraction makes a significant contribution to building up the κ-form crystal structure of (±)-**1c**, and thereby the polymorphic transition of the metastable γ form into the δ form, which would cause preferential enrichment, cannot occur. In fact, the electrostatic potential calculated by using the MNDO/d program in Spartan'02 Windows shows the highly positive cap on the bromine atom in ammonium *p*-bromobenzenesulfonate, which is responsible for the O···Br Coulombic attraction,[21] as depicted in Figure 8.

Thus, it has been proved that such a minor molecular modification exerts a primary influence on the crystal structure.

Induction and inhibition of preferential enrichment: It has been concluded that all of compounds (±)-**1a**–(±)-**1c** predominantly adopt a γ-form supramolecular structure in their supersaturated solutions in EtOH, because 1) the metastable γ-form crystals of (±)-**1c** actually obtained have exhibited the identical S–O stretching vibrations at around $\tilde{\nu}$ = 1190, 1220, and 1240 cm^{-1} both in the solid state and in the supersaturated solution in EtOH as analyzed by in situ attenuated total reflection (ATR) FTIR spectroscopy (Figure 9a,d); 2) (±)-**1a**–(±)-**1c** have shown very similar IR absorptions in the same range of S–O stretching vibrations in their supersaturated solutions in EtOH (Figure 9a); and 3) the analogous IR spectra were also observed for the γ-form molecular assembly of other analogous compounds.[3,7–9] Therefore, it is quite plausible that the incipient formation of the individual metastable γ-form polymorphs and the subsequent polymorphic transition into the stable δ form, δ_1 form, or κ form should have occurred during crystallization of (±)-**1a**, (±)-**1b**, or (±)-**1c** from EtOH, respectively (Table 1). Furthermore, it is noteworthy that 1) the interatomic distance (5.822 Å) between the hydroxy oxygen atom in the *R* chain

 © 2006 Wiley-VCH Verlag GmbH & Co. KGaA, Weinheim

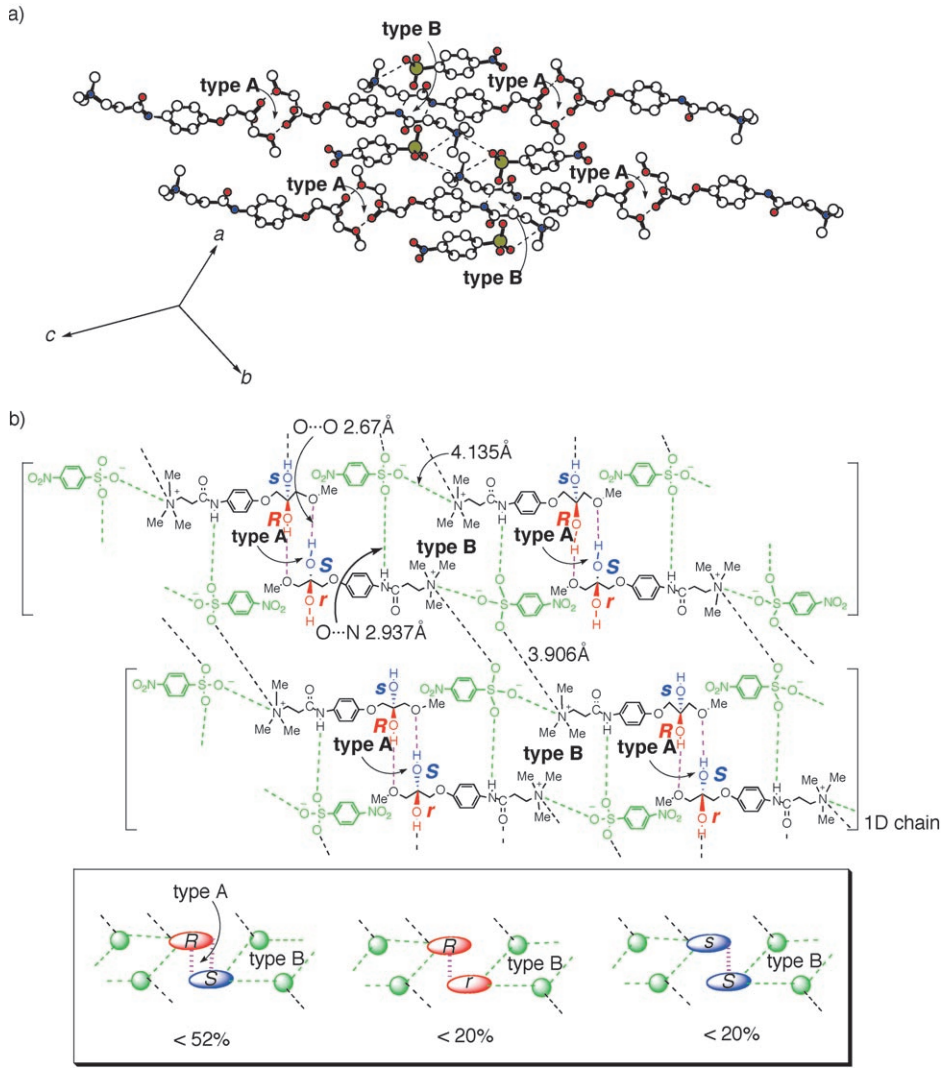

Figure 4. a) Crystal structure of the δ form of (±)-**1a**. The C, O, N, and S atoms are represented by white, red, blue, and yellow circles, respectively. b) Schematic representation of the intermolecular hydrogen bonds in the δ-form crystal. The hydroxy group on the asymmetric carbon atom is disordered over two positions. The *R* and *S* enantiomers in the sites with higher occupancy factor (0.721) are designated *R* and *S*, and those in sites with lower occupancy factor (0.279) *r* and *s*. The ellipsoid and circle in the inset indicate the long-chain cation and sulfonate ion, respectively. The dashed lines show the intermolecular hydrogen bonds and electrostatic interactions. The contents of three dimer structures were estimated from the occupancy factors of the orientationally disordered hydroxy groups.

and the nearest methoxy oxygen atom in the adjacent *S* chain in the γ form of (±)-**1c** seems short enough for further transformation of the γ form into the δ form (Figure 5b);[7] 2) the crystal structure of the δ_1 form of (±)-**1b** has a partial resemblance to that of the δ form of (±)-**1a**, as already stated (Figures 3 and 4); and 3) the δ form of (±)-**1a**, the δ_1 form of (±)-**1b**, and the γ form of (±)-**1c** have a similar columnar structure along one axis (Figure 10a,b,c), suggesting the possibility of forced adsorption of the γ-form prenucleation aggregates of (±)-**1b** or (±)-**1c** on the columnar surface of the δ form of (±)-**1a** and the subsequent polymorphic transition of the incipient γ-form crystalline phase into the desired δ form on the same crystalline surface of (±)-**1a**. Therefore, it is conceivable that preferential enrichment can be induced or inhibited by the alteration of the mode of the polymorphic transition by seeding the crystals with each other. Such has indeed been the case.

The induction of preferential enrichment has been explored for (±)-**1b** and (±)-**1c**, which cannot show preferential enrichment by themselves (Table 1); the respective three- and fivefold supersaturated solutions of (±)-**1b** and (±)-**1c** (0.50 g each) in EtOH (2.5 and 8.5 mL, respectively) were seeded with the δ-form crystals of (±)-**1a** (0.025 g) at −16 °C. Consequently, in the case of (±)-**1b**, whenever more than 3 wt % of the seed crystals were employed, crystallization began quickly and preferential enrichment was distinctly induced (Figure 11 and Table 1). Contrary to expectation, however, DSC and XRD analyses of the deposited crystals showed that the crystal structure is very similar to the δ_1 form (Figures 12b and 13b,c). In fact, the crystal structure has been solved to be a δ_1 form by the same direct-space approach (Table 2, Figure 10e, and Figure S2 in the Supporting Information). It is noteworthy that this δ_1-form crystal structure of nearly racemic **1b** can be solved as either a highly or fairly ordered racemic mixed crystal with a comparable R_{wp} value. These highly and fairly ordered crystal structures are virtually identical; the former has orientationally ordered molecules, while the latter is characterized by the orientational disorder at the position of the hydroxy group on an asymmetric carbon atom with occupancy factors of around 0.7 and 0.3, in which the *R* and *S* enantiomers in sites with higher occupancy factor (0.70) can form the type-A cyclic dimer (O···O distance: 2.853 Å) (see Figure S2 b,c in the Supporting Information). This disordered crystal structure is consistent with the occurrence of preferential enrichment.[5,7,8] Namely, it is easy to conceive that in the crystallization of (±)-**1b** with the δ-form seed crystals of (±)-**1a**, the successive polymorphic transitions from the metastable disordered γ form into the disordered δ

 © 2006 Wiley-VCH Verlag GmbH & Co. KGaA, Weinheim

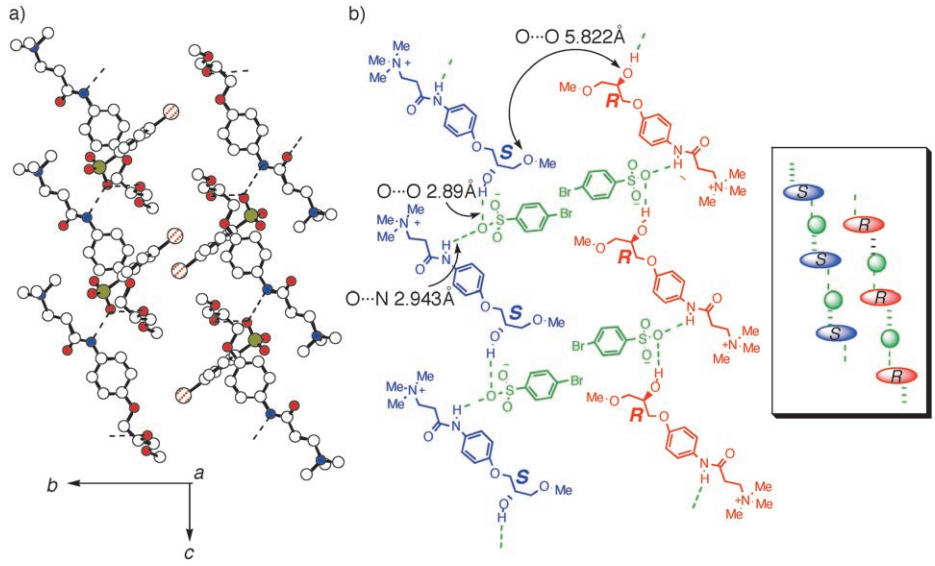

Figure 5. a) Crystal structure of the γ form of (±)-**1c** viewed down the *a* axis. The C, O, N, S, and Br atoms are represented by white, red, blue, yellow, and crosshatched-red circles, respectively. b) Schematic representation of the intermolecular interactions in the crystal. The ellipsoid and circle in the inset indicate the long-chain cation and sulfonate ion, respectively. The dashed lines show the intermolecular hydrogen bonds.

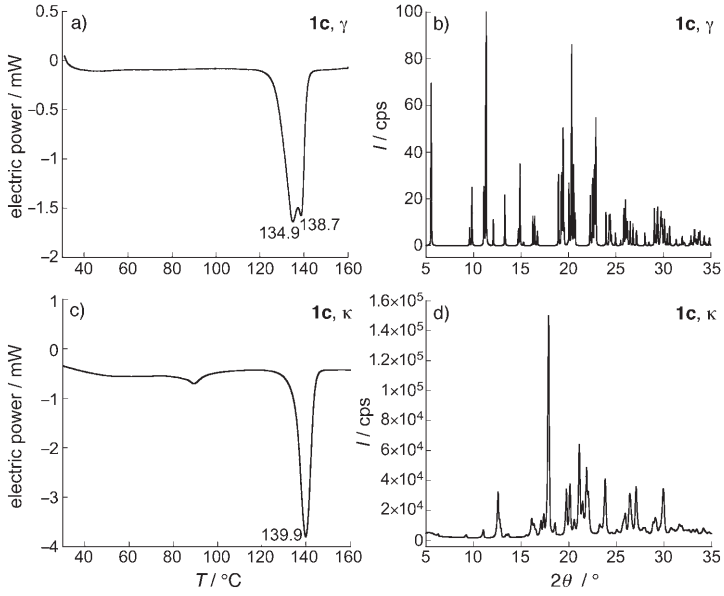

Figure 6. DSC curves and X-ray diffraction patterns of a),b) the thermally unstable γ form of (±)-**1c**, and c),d) the stable κ form of (±)-**1c**, respectively. The DSC curve in a indicates that the γ form is thermally unstable and easily undergoes phase transition by heating to give the κ form. The XRD pattern in b is simulated from the X-ray crystallographic data. In c, the endothermal peak at approximately 90°C corresponds to the deposition of EtOH remaining around the crystals.

form and then the disordered δ_1 form should occur on the columnar surfaces of the δ-form seed crystals, because the occurrence of preferential enrichment has been observed.

Unexpectedly, by seeding the supersaturated solution of (±)-**1c** in EtOH with the δ-form crystals of (±)-**1a**, neither the acceleration of crystallization nor the formation of another polymorphic form has been observed, nor has the induction of preferential enrichment been noted. Instead, more interestingly, seeding with the δ_1-form crystal (5 wt%) of (±)-**1b** in EtOH induced prompt crystallization to provide a new metastable polymorph of **1c** (Figures 6 and 14a,b) and distinctly induced preferential enrichment for (±)-**1c** (Figure 15 and Table 1). The crystal structure of this new polymorph of nearly racemic **1c** has been solved to be a δ_1 form from its powder XDR data by the same direct-space approach (Table 2, Figure 10f, and Figure S3 in the Supporting Information). This δ_1-form crystal structure of (±)-**1c** can be solved only when the orientational disorder with occupancy factors of around 0.7 and 0.3 is assigned to the position of the hydroxy group on an asymmetric carbon atom. Therefore, it is again likely that successive polymorphic transitions from the disordered γ form into the disordered δ form and then the disordered δ_1 form should occur on the columnar surface of the δ_1-form seed crystal of (±)-**1b**. This is a rather interesting example of the successful induction of preferential enrichment by using the seed crystals of another compound that cannot show this phenomenon by itself.

Conversely, the occurrence of preferential enrichment of (±)-**1a** in EtOH has been completely inhibited by seeding with the δ_1-form crystals (more than 3 wt%) of (±)-**1b** (Table 1); this indicates a drastic change of the mode of the polymorphic transition on the columnar surfaces of the seed crystals, as confirmed by DSC analysis and XRD measurements of the deposited crystals (Figures 12a, 13a, and 14c,d). The crystal structure of this new polymorph of (±)-**1a**, which is thermally less stable than the δ form, has turned out to be a δ_1 form from its powder XDR data by using the same direct-space approach (Table 2, Figure 10d, and Figure S4 in the Supporting Information). But in the δ_1 form of (±)-**1a**, there is no C(sp^2)H···O contact between the oxygen atom of the nitro group and the hydrogen atoms on the benzene ring of the neighboring long-chain cation.

Thus, it is most likely that in the crystallization of (±)-**1a** with the δ_1-form seed crystals of (±)-**1b**, a single-phase transition from the γ form into the δ_1 form should occur on the columnar surfaces of the δ_1-form seed crystals, because preferential enrichment has been inhibited by seeding.

Mode of the polymorphic transition on crystalline surfaces: With respect to the compounds showing preferential enrichment by themselves, such as (±)-**1a** and (±)-**2a**–(±)-**2c**, ad-

 © 2006 Wiley-VCH Verlag GmbH & Co. KGaA, Weinheim

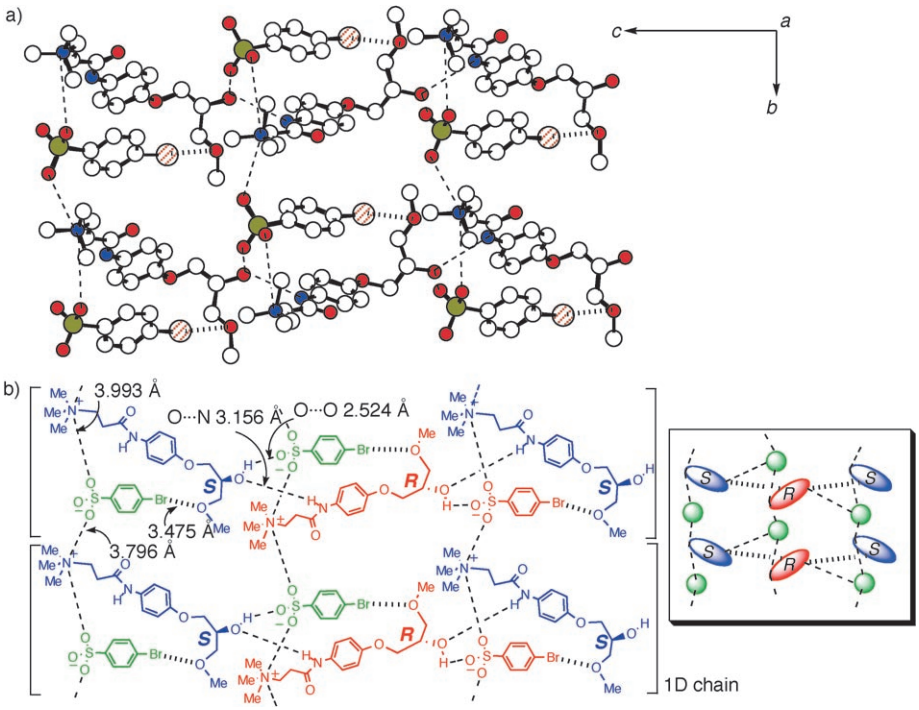

Figure 7. a) Crystal structure of the κ form of (±)-**1c** viewed down the *a* axis. The C, O, N, S, and Br atoms are represented by white, red, blue, yellow, and crosshatched-red circles, respectively. b) Schematic representation of the intermolecular interactions in the crystal. The ellipsoid and circle in the inset indicate the long-chain cation and sulfonate ion, respectively.

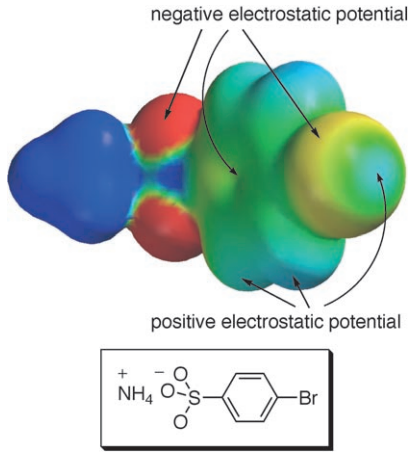

Figure 8. Plot showing the electrostatic potential of ammonium *p*-bromobenzenesulfonate calculated using the MNDO/d program in Spartan'02 Windows. The positive cap on the bromine atom is distinctly seen.

dition of the individual seed crystals to their own supersaturated solutions in EtOH has been found to induce prompt crystallization and thereby accelerate the rate of preferential enrichment (Table 1). This acceleration effect can be accounted for by an "epitaxial transition", that is, 1) the adsorption of the γ-form prenucleation aggregates, 2) the heterogeneous nucleation and crystal growth of the incipient metastable γ-form polymorph, and 3) the subsequent polymorphic transition into the more stable δ form; these three processes occur on the same surface of the δ-form crystalline substrate (Figure 16).

Likewise, in the mechanism of preferential enrichment induced by seeding a supersaturated solution of (±)-**1b** or (±)-**1c** in EtOH with the δ form of (±)-**1a** or the δ_1 form of (±)-**1b**, respectively, a similar epitaxial transition process must operate (Figure 16).

The unexpected induction of the preferential enrichment of (±)-**1c** by the δ_1-form seed crystals of (±)-**1b** can be accounted for by the moderate affinity of the γ-form prenucleation aggregates of (±)-**1c** toward the *bc* plane of the δ_1-form crystal of (±)-**1b** (Figure 10b,c). The occurrence of preferential enrichment indicates the initial polymorphic transition of the disordered γ form into the disordered δ form on a surface of the δ_1-form seed crystal of (±)-**1b**. And the subsequent, fairly fast polymorphic transition process from the resulting δ form into the

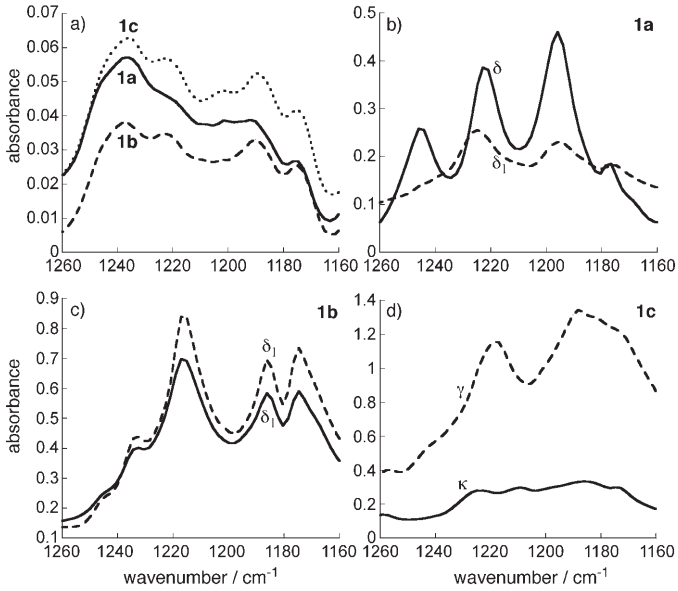

Figure 9. ATR-FTIR spectra monitored a) in the supersaturated solutions of (±)-**1a** (——), (±)-**1b** (– – –), and (±)-**1c** (•••••) in EtOH, and in the solid state of b) the δ form (——) and δ_1 form (– – –) of (±)-**1a**, c) the δ_1 form of (±)-**1b** crystallized with (– – –) and without (——) the seed crystals (5 wt %) of the δ form of (±)-**1a**, and d) the γ form (– – –) and κ form (——) of (±)-**1c**.

 © 2006 Wiley-VCH Verlag GmbH & Co. KGaA, Weinheim

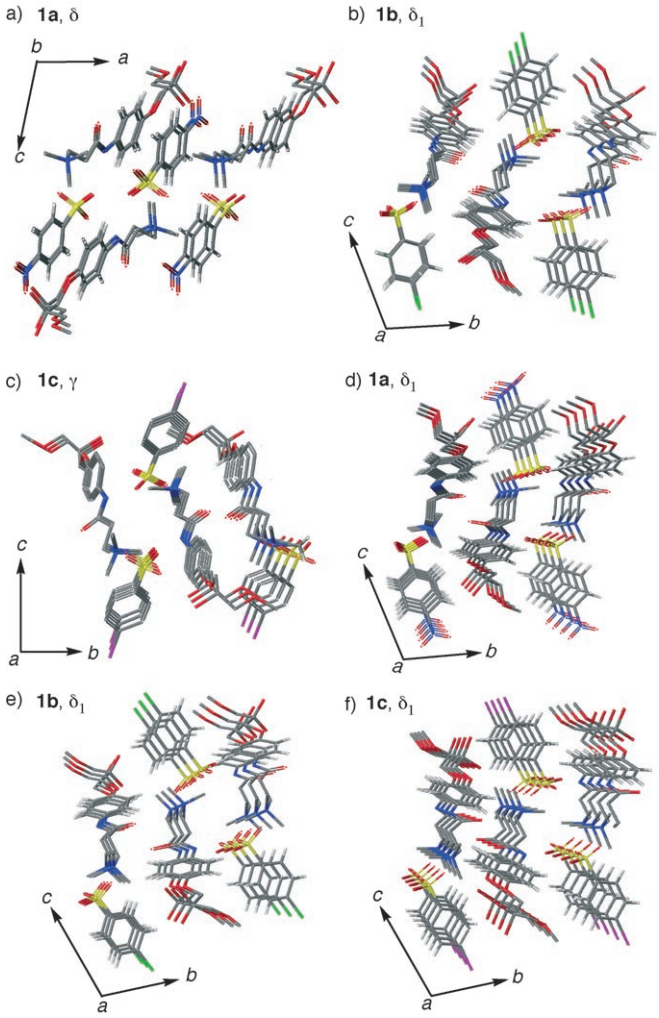

Figure 10. Similar columnar crystal structures of a) the δ form of (±)-**1a** viewed down the *b* axis, b) the δ_1 form of (±)-**1b**, crystallized without seed crystals, viewed down the *a* axis, c) the γ form of (±)-**1c** viewed down the *a* axis, d) the δ_1 form of (±)-**1a** viewed down the *a* axis, e) the δ_1 form of (±)-**1b**, crystallized with seed crystals (5 wt%) of the δ form of (±)-**1a**, viewed down the *a* axis, and f) the δ_1 form of (±)-**1c** viewed down the *a* axis. The C, O, N, S, Cl, and Br atoms are represented by gray, red, blue, yellow, green, and purple sticks, respectively. All H atoms in c are omitted.

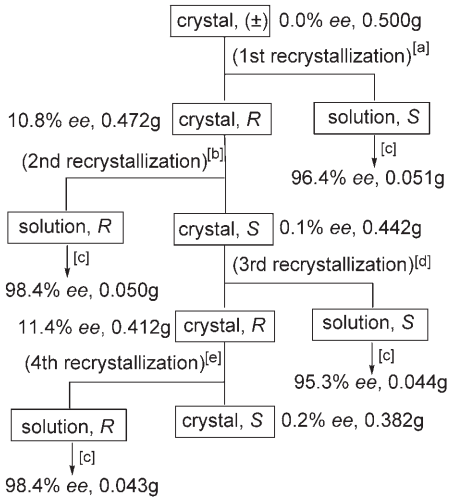

Figure 11. Preferential enrichment of (±)-**1b** induced by seeding with the δ-form crystals of (±)-**1a** (5 wt%) in EtOH. Conditions: [a] In EtOH (2.5 mL) with 0.025 g of (±)-**1a** at −16 °C for 7 days. [b] In EtOH (2.4 mL) with 0.024 g of (±)-**1a** at −16 °C for 7 days. [c] Removal of the solvent by evaporation. [d] In EtOH (2.20 mL) with 0.021 g of (±)-**1a** at −16 °C for 7 days. [e] In EtOH (2.0 mL) 0.020 g of (±)-**1a** at −16 °C for 7 days.

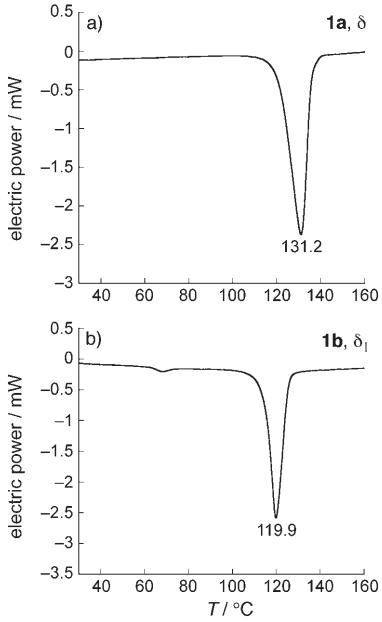

Figure 12. DSC curves of a) the δ form of (±)-**1a** and b) the δ_1 form of (±)-**1b** obtained by crystallization with seed crystals (5 wt%) of the δ form of (±)-**1a** from EtOH at −16 °C. In b, the endothermal peak at approximately 70 °C corresponds to the deposition of EtOH remaining around the crystals.

more stable δ_1 form before completion of the crystal disintegration in the disordered δ form must be responsible for the moderate *ee* value (33.2–66.8% *ee*) reached in solution after each recrystallization operation (Figure 15).

In contrast, it is clear that no adsorption of the γ-form prenucleation aggregates of (±)-**1c** on the canted *ac* plane of the δ-form crystal of (±)-**1a** (Figure 10a,c) occurs, most likely due to the lattice mismatching (Table 2), which results in the homogeneous nucleation of the γ form of (±)-**1c** and its direct polymorphic transformation into the most stable κ form, irrespective of the presence of the δ-form seed crystals of (±)-**1a**.

Similarly, the mechanism of inhibition of preferential enrichment by seeding the supersaturated solution of (±)-**1a** in EtOH with the δ_1 form of (±)-**1b** must exclusively involve the direct transformation of the incipient γ form into the stable δ_1 form without passing through the δ form, due to the good lattice matching between the γ-form prenucleation aggregates of (±)-**1a** and the crystal surface of the δ_1 form of (±)-**1b** (Figure 10b,d).

 © 2006 Wiley-VCH Verlag GmbH & Co. KGaA, Weinheim

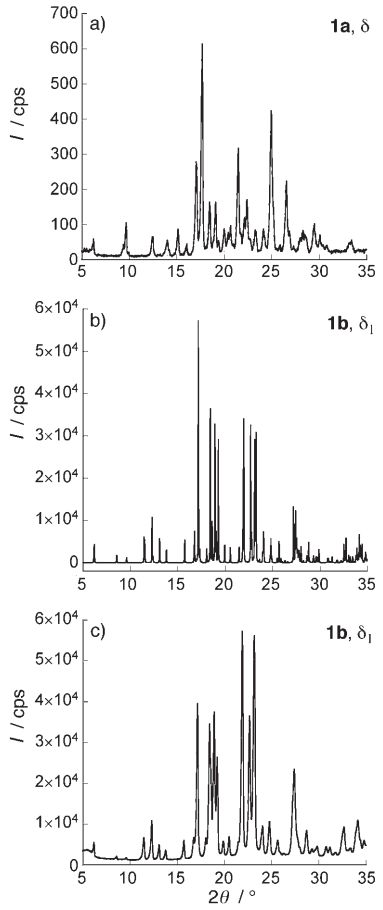

Figure 13. X-ray diffraction patterns of the crystals of a) the δ form of (±)-**1a** and b) the δ_1 form of (±)-**1b**, crystallized without seed crystals from *i*PrOH at 25 °C, and c) the δ_1 form of (±)-**1b**, crystallized with seed crystals (5 wt %) of the δ form of (±)-**1a** from EtOH at −16 °C. The XRD pattern in b is simulated from the X-ray crystallographic data.

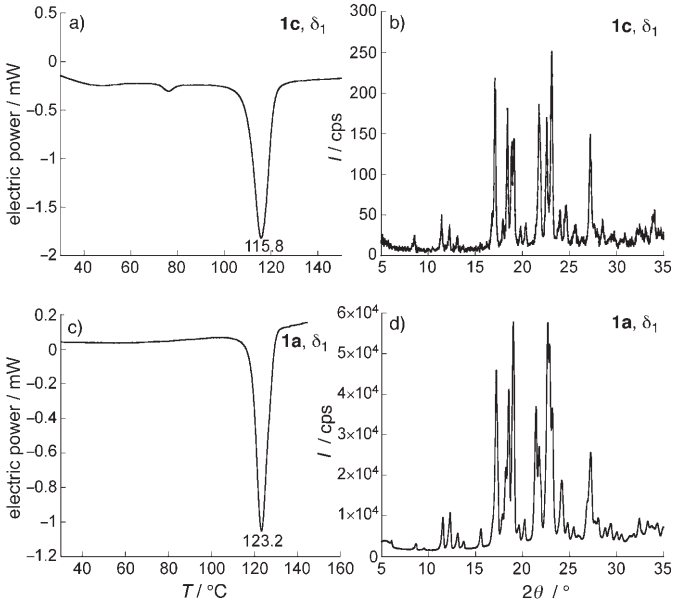

Figure 14. a) DSC curve and b) X-ray diffraction pattern of the δ_1-form crystals obtained by crystallization of (±)-**1c** from EtOH in the presence of seed crystals (5 wt %) of the δ_1 form of (±)-**1b** at −16 °C. c) DSC curve and d) X-ray diffraction pattern of the δ_1-form crystals of (±)-**1a** obtained by seeding the supersaturated solution of (±)-**1a** in EtOH with the δ_1 form of (±)-**1b** (5 wt %) at −16 °C. In a, the endothermal peak at approximately 70 °C corresponds to the deposition of EtOH remaining around the crystals.

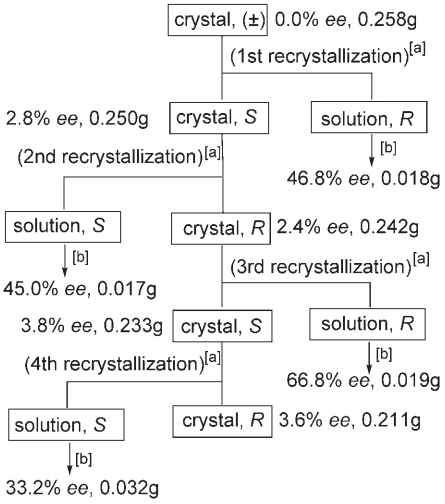

Figure 15. Preferential enrichment of (±)-**1c** induced by seeding with the δ_1-form crystals of (±)-**1b** (5 wt %) in EtOH. Conditions: [a] In EtOH (1.4 mL) with 0.013 g of (±)-**1b** at −16 °C for 24 h. [b] Removal of the solvent by evaporation.

Accordingly, these are the distinct examples of an "epitaxial transition". Thus, it has been proved that by seeding with each other, the two compounds showing the good lattice and crystal-structure matching such as (±)-**1a** and (±)-**1b** can strongly affect the mutual mode of the polymorphic transition occurring on the crystalline surface during crystallization.

Conclusion

We have described some examples in which slight molecular modification in a series of racemic substances largely affects the mode of polymorphic transition during crystallization from solution, resulting in the formation of stable crystals with different crystal structures. In this case, if the crystal lattices and crystal structures of the two compounds are partly similar to each other, it is possible to control the mode of polymorphic transition mutually by seeding them with each other. By using this methodology, preferential enrichment has been successfully induced for certain racemic samples that cannot show preferential enrichment by themselves. Furthermore, the phenomenon of preferential enrichment has turned out to be usable as an excellent probe to detect the occurrence of an epitaxial transition process on a crystalline surface. In addition, it should be stressed that the crystal-structure solution from the powder X-ray diffraction data using the direct-space approach is essential for eluci-

 © 2006 Wiley-VCH Verlag GmbH & Co. KGaA, Weinheim

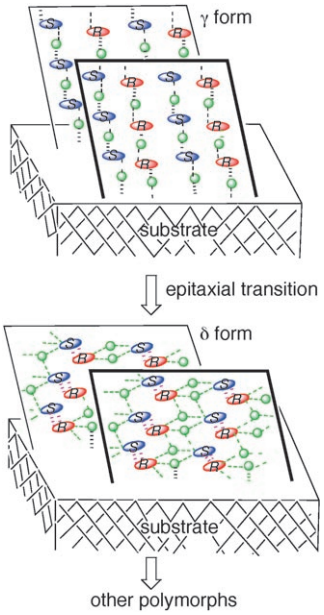

Figure 16. Schematic representation of the epitaxial transition of the metastable γ-form polymorph into the δ form causing preferential enrichment on the surface of a δ- or δ_1-form crystalline substrate.

dating the mechanism of the polymorphic transition occurring during crystallization, because it is not an easy task to produce the single crystal with the same crystal structure as the powder sample obtained after a solid-to-solid type of polymorphic transition.

Experimental Section

General: Differential scanning calorimetry (DSC) experiments were performed at the scanning rate of 5 °C min^{-1}. The in situ FTIR spectra in solution or suspension and the solid-state FTIR spectra were recorded by using the ATR method on a ReactIR 4000 spectrometer. ^{1}H NMR spectra were recorded at 270 MHz at 25 °C using tetramethylsilane (TMS) as an internal standard, and ^{13}C NMR spectra were recorded at 67.8 MHz under the same conditions. HPLC analyses were performed by using a chiral stationary-phase column (Daicel Chiralcel OD-H, 0.46×25 cm), a mixture of hexane, ethanol, trifluoroacetic acid, and diethylamine (800:200:5:1) as the mobile phase at a flow rate of 0.5 mL min^{-1}, and a UV/Vis spectrometer (254 nm) as the detector.[22] Powder X-ray diffraction patterns were recorded at a continuous scanning rate of 2° 2θ min^{-1} (0.02° min^{-1} for structure solution) using $Cu_{K\alpha}$ radiation (40 kV, 20 mA) with the intensity of diffracted X-rays being collected at intervals of 2θ = 0.02° (0.01° for structure solution). A Ni filter was used to remove $Cu_{K\beta}$ radiation. Compounds (±)-**1a** and (±)-**1c** were prepared in a similar way to the procedure used for the preparation of (±)-**1b**.[4]

Compound (±)-1a: ^{1}H NMR (CD_3OD): δ = 2.94 (t, ^3J(H,H) = 7.6 Hz, 2H), 3.17 (s, 9H), 3.38 (s, 3H), 3.51–3.54 (m, 2H), 3.74 (t, ^3J(H,H) = 7.6 Hz, 2H), 3.94–4.05 (m, 3H), 6.90 (d, ^3J(H,H) = 8.9 Hz, 2H), 7.43 (d, ^3J(H,H) = 8.9 Hz, 2H), 8.01 (d, ^3J(H,H) = 8.9 Hz, 2H), 8.26 ppm (d, ^3J(H,H) = 8.9 Hz, 2H); ^{13}C NMR (CD_3OD): δ = 31.0, 53.7, 59.4, 69.8, 70.6, 74.7, 78.9, 115.5, 122.6, 124.4, 128.0, 132,3, 149.7, 152.0, 156.9, 168.0 ppm; IR (KBr): $\tilde{\nu}$ = 3384, 2937, 2360, 1868, 1683, 1608, 1541, 1514, 1488, 1417, 1226, 1203, 1122, 1033, 1010 cm^{-1}; elemental analysis calcd (%) for $C_{22}H_{31}N_3O_7S$: C 51.45, H 6.08, N 8.18; found: C 51.18, H 6.14, N 7.89.

Compound (±)-1c: ^{1}H NMR (CD_3OD): δ = 2.94 (t, ^3J(H,H) = 7.3 Hz, 2H), 3.17 (s, 9H), 3.38 (s, 3H), 3.51–3.54 (m, 2H), 3.74 (t, ^3J(H,H) = 7.3 Hz, 2H), 3.93–4.04 (m, 3H), 6.91 (d, ^3J(H,H) = 8.9 Hz, 2H), 7.43 (d, ^3J(H,H) = 8.9 Hz, 2H), 7.57 (d, ^3J(H,H) = 8.6 Hz, 2H), 7.72 ppm (d, ^3J(H,H) = 8.6 Hz, 2H); ^{13}C NMR (CD_3OD): δ = 31.2, 53.8, 63.5, 70.2, 70.8, 72.3, 74.2, 115.7, 122.8, 126.8, 129.8, 132.6, 141.6, 143.4, 157.1, 168.2 ppm; IR (KBr): $\tilde{\nu}$ = 3566, 2934, 2361, 1684, 1541, 1508, 1473, 1191, 1124, 1035, 1010 cm^{-1}; elemental analysis calcd (%) for $C_{22}H_{31}BrN_2O_7S$: C 48.27, H 5.71, N 5.12; found: C 47.99, H 5.85, N 5.01.

Enantiopure **1a**, **1b**, and **1c** were similarly synthesized from (*S*)-methyl glycidyl ether and used as authentic samples for HPLC analysis. (*R*)-**1a**: $[\alpha]_D^{22}$ = −1.02(2) (*c* = 0.998 in MeOH); (*R*)-**1b**: $[\alpha]_D^{22}$ = −2.68(11) (*c* = 0.998 in MeOH); (*R*)-**1c**: $[\alpha]_D^{22}$ = −3.84(32) (*c* = 0.994 in MeOH).

Preferential-enrichment experiment of (±)-1a (Figure 2): Compound (±)-**1a** (0.500 g, 0.975 mmol; 0.244 mol L^{-1}) was dissolved in EtOH (4.0 mL) on heating. The resulting supersaturated (ca. 10-fold) solution was stirred at 25 °C until crystallization began, and was then allowed to stand at 25 °C for 1 day and then at 5 °C for 4 days. The deposited crystals were separated from the mother liquor by using filtration. From the *R*-rich solution, **1a** (0.043 g, 87.2 % *ee*) was obtained as a viscous yellow oil after evaporation of the solvent. The deposited *S*-rich crystals (0.453 g, 9.2 % *ee*) were subsequently recrystallized from EtOH (3.5 mL) in a similar way, leading to the deposition of antipodal *R*-rich crystals (0.399 g, 1.0 % *ee*) and an enrichment of the *S* enantiomer in the mother liquor, from which *S*-rich **1a** (0.050 g, 98.4 % *ee*) was obtained as a viscous oil. Similar crystallizations were repeated four times in all.

Induced preferential-enrichment experiment by seeding the supersaturated solution of (±)-1b in EtOH with the δ-form crystals of (±)-1a (Figure 11): Compound (±)-**1b** (0.500 g, 0.994 mmol; 0.398 mol L^{-1}) was dissolved in EtOH (2.5 mL) on heating. After cooling the sample to 25 °C, finely powdered δ-form crystals (0.025 g) of (±)-**1a** were added to the supersaturated (ca. 3-fold) solution. After being allowed to stand at −16 °C for 7 days, the deposited *R*-rich crystals (0.472 g, 10.8 % *ee*) were separated from the mother liquor by using filtration. From the *S*-rich solution, **1b** (0.051 g, (96.4 % *ee*) was obtained as a viscous colorless oil after evaporation of the solvent. Similar crystallizations were repeated four times in all. In this case, because the molecular structures of the cationic portions are the same for **1a** and **1b**, we did not purify the deposited crystals of **1b** containing a small amount of **1a** after each recrystallization. After four consecutive recrystallizations, the added **1a** was not detected in the mother liquor but was observed in the deposited crystals by ^{1}H NMR spectroscopic analysis. When purification of the deposited **1b** was necessary, it was achieved by simply removing the yellow portions of (±)-**1a** in the deposited crystals by using a spatula.

The induced-preferential-enrichment experiment by seeding the supersaturated solution of (±)-**1c** in EtOH with the δ_1-form crystal of (±)-**1b** was similarly carried out (Figure 15).

X-ray crystallographic analysis of the δ form of (±)-1a and the γ form of (±)-1c: For the X-ray crystallographic analysis, the single crystal was mounted in a sealed capillary. The data collections were performed at 293 K on an Enraf-Nonius CAD4 diffractometer with graphite-monochromated $Cu_{K\alpha}$ radiation for the δ form of (±)-**1a** and an Enraf-Nonius Kapp CCD diffractometer with graphite-monochromated $Mo_{K\alpha}$ radiation for the γ form of (±)-**1c**. All of the crystallographic calculations were performed by using the CrystalStructure software package of Rigaku and Rigaku/MSC. The crystal structures were solved by direct methods and refined by using full-matrix least squares. All non-hydrogen atoms were refined anisotropically. The summary of the fundamental crystal data and experimental parameters for the structure determination is given in Table 2. The experimental details including data collection, data reduction, and structure solution and refinement, as well as the atomic coordinates, Biso/Beq values, and anisotropic displacement parameters, have been deposited in the Supporting Information.

CCDC-270808 and -270809 contain the supplementary crystallographic data for this paper. These data can be obtained free of charge from the Cambridge Crystallographic Data Centre via www.ccdc.cam.ac.uk/data_request/cif.

 © 2006 Wiley-VCH Verlag GmbH & Co. KGaA, Weinheim

Crystal structure solution from powder X-ray diffraction data of the δ_1 form of (±)-1a, the δ_1 form of (±)-1b, and the κ and δ_1 forms of (±)-1c (Table 2): For all calculations, a software module Reflex Plus implemented in Materials Studio, which includes the following software, was used.[23] The COMPASS force field was used for energy calculations.[24]

The powder patterns of the δ_1 form of (±)-**1a** and the κ form of (±)-**1c** were indexed by the X-cell program[25] using 30 reflections ($2\theta < 42°$). Systematic absences, impurity peaks, and zero-point correction were taken into account to establish a complete list of all possible indexing solutions. Among 2578 or 3043 solutions obtained for the δ_1 or κ form, respectively, a top-ranked solution retained relative figures of merit of 0.920 or 1.487, respectively, zero-point shift of 0.01975 or −0.00660, respectively, and no impurity peaks; to state the conclusion first, the top-ranked solution, assigned to space group $P\bar{1}$ (No. 2) ($Z=2$) or $P2_1/c$ (No. 14) ($Z=4$), respectively, led to the successful elucidation of the crystal structure.

The powder patterns of the δ_1 form of (±)-**1b** and the δ_1 form of (±)-**1c** were indexed by the TREOR90 program[26] using 29 and 30 reflections ($2\theta < 42°$), respectively; the figures of merit ($F(29)$ and $F(30)$) for the best solution were 19 and 22, respectively. The obtained cell and the function profile parameters were refined by using the Pawley method (data range: $2° < 2\theta < 42°$) and used.[27] The space groups were determined to be $P\bar{1}$ (No. 2) ($Z=2$) by means of a trial and error method using the Pawley method among the space-group candidates consistent with systematic absences.

After the initial model molecular conformation of the δ_1 form of (±)-**1a**, the δ_1 form of (±)-**1b**, the κ form of (±)-**1c**, or the δ_1 form of (±)-**1c** was assigned, the subsequent structure solution was carried out by using the Monte Carlo/parallel tempering method with the software Powder-Solve.[19,23] In the case of the δ_1 form of (±)-**1c**, the reasonable crystal structure with a sufficiently low R_{wp} value was obtained only when the occupancy factors (around 0.70 and 0.30) were assigned to the position of the hydroxy group on an asymmetric carbon atom. For the δ_1 form of (±)-**1b**, the reasonable crystal structure with a sufficiently low R_{wp} value was obtained when the occupancy factors (0.70 and 0.30) or (1.00 and 0) were assigned to the position of the hydroxy group; the two crystal structures are very similar except that the former has the orientationally disordered hydroxy groups. For the refinement of atomic positions inside the crystal, all atoms of each ionic molecule were assigned to one motion group so that the atoms were not allowed to move independently and they were translated and rotated as part of the motion group. Inside an asymmetric unit, seven single bonds with variable torsional angles have been defined in the long-chain cation so as to limit the total degrees of freedom to nineteen: seven for these defined torsional angles and another six (three translations and three rotations) each for the two ionic motion groups (Scheme 1). For the subsequent Rietveld refinement,[28] the following conditions were applied: 1) the pseudo-Voight function was used for simulating the peak shape; 2) the background was determined by linear interpolation using 20 terms; 3) the Berar–Baldinozzi method was used for asymmetric refinement; 4) the March–Dollase method was applied to correct the effects of preferred orientation. For the refinement of temperature factors, global isotropic factors were used, because the powder diffraction pattern does not contain enough information to use more accurate atomic temperature factors. Inside each of the motion groups, the molecular conformation was refined by varying the torsional angles around all single bonds. The Monte Carlo calculations with the subsequent Rietveld refinement were repeated until the R_{wp} value became below 0.20 and constant.

Acknowledgements

The present work was supported by the Grant-in-Aid for Scientific Research (No. 15350023) from Japan Society for the Promotion of Science. We thank Dr. Takanori Ushio, Taiho Pharmaceutical Co. Ltd., for helpful discussions.

[1] a) T. Ushio, R. Tamura, H. Takahashi, N. Azuma, K. Yamamoto, *Angew. Chem.* **1996**, *108*, 2544–2546; *Angew. Chem. Int. Ed. Engl.* **1996**, *35*, 2372–2374; b) T. Ushio, R. Tamura, N. Azuma, K. Nakamura, F. Toda, K. Kobayashi, *Mol. Cryst. Liq. Cryst. Sect. A* **1996**, *276*, 245–252.

[2] R. Tamura, H. Takahashi, K. Hirotsu, Y. Nakajima, T. Ushio, F. Toda, *Angew. Chem.* **1998**, *110*, 3002–3005; *Angew. Chem. Int. Ed.* **1998**, *37*, 2876–2878.

[3] D. Fujimoto, R. Tamura, Z. Lepp, H. Takahashi, T. Ushio, *Cryst. Growth Des.* **2003**, *3*, 973–979.

[4] R. Tamura, H. Takahashi, H. Miura, Z. Lepp, Y. Nakajima, K. Hirotsu, T. Ushio, *Supramol. Chem.* **2001**, *13*, 71–78.

[5] H. Takahashi, R. Tamura, D. Fujimoto, Z. Lepp, K. Kobayashi, T. Ushio, *Chirality* **2002**, *14*, 541–547.

[6] a) R. Tamura, T. Ushio, H. Takahashi, K. Nakamura, N. Azuma, F. Toda, K. Endo, *Chirality* **1997**, *9*, 220–224; b) R. Tamura, T. Ushio, K. Nakamura, H. Takahashi, N. Azuma, F. Toda, *Enantiomer* **1997**, *2*, 277–280; c) H. Takahashi, R. Tamura, T. Ushio, Y. Nakajima, K. Hirotsu, *Chirality* **1998**, *10*, 705–710; d) R. Tamura, H. Takahashi, T. Ushio, Y. Nakajima, K. Hirotsu, F. Toda, *Enantiomer* **1998**, *3*, 149–157; e) H. Takahashi, R. Tamura, Z. Lepp, K. Kobayashi, T. Ushio, *Enantiomer* **2001**, *6*, 57–66; f) R. Tamura, H. Takahashi, K. Hirotsu, Y. Nakajima, T. Ushio, *Mol. Cryst. Liq. Cryst. Sect. A* **2001**, *356*, 185–194; g) H. Takahashi, R. Tamura, S. Yabunaka, T. Ushio, *Mendeleev Commun.* **2003**, 119–121.

[7] R. Tamura, D. Fujimoto, Z. Lepp, K. Misaki, H. Miura, H. Takahashi, T. Ushio, T. Nakai, K. Hirotsu, *J. Am. Chem. Soc.* **2002**, *124*, 13139–13153.

[8] R. Tamura, T. Ushio in *Enantiomer Separation: Fundamentals and Practical Methods* (Ed.: F. Toda), Kluwer Academic Publishers, Dortrecht, **2004**, pp. 135–163.

[9] H. Miura, T. Ushio, K. Nagai, D. Fujimoto, Z. Lepp, H. Takahashi, R. Tamura, *Cryst. Growth Des.* **2003**, *3*, 959–965.

[10] a) W. Ostwald, *Grundriss der Allgemeinen Chemie*, Leipzig, **1899**; b) W. C. McCrone in *Physics and Chemistry of the Organic Solid State, Vol. 2* (Eds.: D. Fox, M. M. Labes, A. Weissberger), Interscience, New York, **1965**, pp. 726–767; c) J. D. Dunitz, J. Bernstein, *Acc. Chem. Res.* **1995**, *28*, 193–200; d) *Polymorphism in Pharmaceutical Solids, Drugs and the Pharmaceutical Sciences, Vol. 95* (Ed.: H. G. Brittain), Marcel Dekker, New York, **1999**; e) J. Bernstein, R. J. Davey, J.-o. Henck, *Angew. Chem.* **1999**, *111*, 3646–3669; *Angew. Chem. Int. Ed.* **1999**, *38*, 3440–3461; f) J. Bernstein, *Polymorphism in Molecular Crystals*, Oxford University Press, Oxford, **2002**.

[11] a) S. Maruyama, H. Ooshima, *J. Cryst. Growth* **2000**, *212*, 239–245; b) M. Kitamura, S. Ueno, K. Sato in *Crystallization Processes* (Ed.: H. Ohtaki), Wiley, Chichester, **1998**, pp. 99–129; c) M. Kitamura, *J. Cryst. Growth* **1989**, *96*, 541–546.

[12] a) M. D. Ward, S. J. Bonafede, A. C. Hiller in *A Modular Chemistry, NATO ASI Ser., Ser. C, Vol. 499* (Ed.: J. Michl), Kluwer Academic Publishers, Dordrecht, **1997**, pp. 637–649; b) D. E. Hooks, T. Fritz, M. D. Ward, *Adv. Mater.* **2001**, *13*, 227–241; c) S. J. Bonafede, M. D. Ward, *J. Am. Chem. Soc.* **1995**, *117*, 7853–7861; d) C. A. Mitchell, L. Yu, M. D. Ward, *J. Am. Chem. Soc.* **2001**, *123*, 10830–10839.

[13] a) I. Weisbuch, L. Leiserowitz, M. Lahav in *Crystallization Technology Handbook* (Ed.: A. Mersmann), Marcel Dekker, New York, **1995**, pp. 401–457; b) R. J. Davey, N. Blagden, G. D. Potts, R. Docherty, *J. Am. Chem. Soc.* **1997**, *119*, 1767–1772; c) N. Blagden, R. J. Davey, R. Rowe, R. Roberts, *Int. J. Pharm.* **1998**, *172*, 169–177.

[14] a) H. Koshima, M. Miyauchi, *Cryst. Growth Des.* **2001**, *1*, 355–357; b) H. Koshima, S. Honke, M. Miyauchi, *Enantiomer* **2000**, *5*, 125–127.

[15] a) E. A. Stura, I. A. Wilson, *J. Cryst. Growth* **1991**, *110*, 270–282; b) E. A. Stura, J.-b. Charbonnier, M. J. Taussig, *J. Cryst. Growth* **1999**, *196*, 250–260.

[16] For in situ monitoring of general solvent-mediated polymorphic transitions, see: B. O'Sullivan, P. Barett, G. Hsiao, A. Carr, B. Glennon, *Org. Process Res. Dev.* **2003**, *7*, 977–982.

 © 2006 Wiley-VCH Verlag GmbH & Co. KGaA, Weinheim

[17] For the mechanism of crystallization at the air–liquid interface, see: a) H. Rapaport, I. Kuzmenko, M. Berfeld, K. Kjaer, J. Als-Nielsen, R. Popovitz-Biro, I. Weisbuch, M. Lahav, L. Leiserowitz, *J. Phys. Chem. B* **2000**, *104*, 1399–1428; b) H. Rapaport, I. Kuzmenko, S. Lafont, K. Kjaer, P. B. Howes, J. Als-Nielsen, M. Lahav, L. Leiserowitz, *Biophys. J.* **2001**, *81*, 2729–2736; c) I. Solomonov, M. J. Weygand, K. Kjaer, H. Rapaport, L. Leiserowitz, *Biophys. J.* **2005**, *88*, 1809–1817.

[18] a) G. R. Desiraju, T. Steiner, *The Weak Hydrogen Bond*, Oxford University Press, Oxford, **1999**; b) G. R. Desiraju, *Acc. Chem. Res.* **2002**, *35*, 565–573; c) A. Nangia, *CrystEngComm* **2002**, *4*, 93–101; d) J. N. Moorthy, R. Natarajan, P. Mal, P. Venugopalan, *J. Am. Chem. Soc.* **2002**, *124*, 6530–6531.

[19] a) K. D. M. Harris, M. Tremayne, P. Lightfoot, P. G. Bruce, *J. Am. Chem. Soc.* **1994**, *116*, 3543–3547; b) G. E. Engel, S. Wilke, O. Konig, K. D. M. Harris, F. J. J. Leusen, *J. Appl. Crystallogr.* **1999**, *32*, 1169–1179; c) G. A. Stephenson, *J. Pharm. Sci.* **2000**, *89*, 958–966.

[20] For reviews, see: a) K. D. M. Harris, M. Tremayne, B. M. Kariuki, *Angew. Chem.* **2001**, *113*, 1674–1700; *Angew. Chem. Int. Ed.* **2001**, *40*, 1626–1651; b) *Structure Determination from Powder Diffraction Data* (Eds.: W. I. F. David, K. Shankland, L. B. McCusker, Ch. Baerlocher), Oxford University Press, Oxford, **2002**; c) K. D. M. Harris, *Cryst. Growth Des.* **2003**, *3*, 887–895; d) K. D. M. Harris, E. Y. Cheung, *Org. Process Res. Dev.* **2003**, *7*, 970–976.

[21] J. P. M. Lommerse, A. J. Stone, R. Taylor, F. H. Allen, *J. Am. Chem. Soc.* **1996**, *118*, 3108–3116.

[22] T. Ushio, K. Yamamoto, *J. Chromatogr. A* **1994**, *684*, 235–242.

[23] Materials Studio (version 2.2), Accelrys Inc., San Diego, **2002**.

[24] a) H. Sun, *J. Phys. Chem. B* **1998**, *102*, 7338–7364; b) COMPASS was distributed along with Materials Studio in ref. [23].

[25] M. Neumann, *J. Appl. Crystallogr.* **2003**, *36*, 356–365.

[26] P. E. Werner, L. Eriksson, M. Westdahl, *J. Appl. Crystallogr.* **1985**, *18*, 367–370.

[27] G. S. Pawley, *J. Appl. Crystallogr.* **1981**, *14*, 357–361.

[28] a) H. M. Rietveld, *J. Appl. Crystallogr.* **1969**, *2*, 65–71; b) *The Rietveld Method, IUCr Monographies of Crystallography 5* (Ed.: R. A. Young), Oxford University Press, Oxford, **1993**.

Received: May 4, 2005
Revised: December 7, 2005
Published online: February 27, 2006

 © 2006 Wiley-VCH Verlag GmbH & Co. KGaA, Weinheim